An International Journal of Optimization and Control: Theories & Applications
ISSN: 2146-0957 eISSN: 2146-5703
Vol.15, No.3, pp.464-482 (2025)
https://doi.org/10.36922/IJOCTA025120054

RESEARCH ARTICLE

Application of Jumarie-Stancu Collocation Series Method and Multi-Step Generalized Differential Transform Method to fractional glucose-insulin

Sayed Saber[1,2*], Brahim Dridi[3], Abdullah Alahmari[3], and Mohammed Messaoudi[4]

[1]Department of Mathematics, Faculty of Science, Al-Baha University, Al-Baha, Saudi Arabia
[2]Department of Mathematics and Computer Science, Faculty of Science, Beni-Suef University, Egypt
[3]Department of Mathematics, Faculty of Sciences, Umm Al-Qura University, Saudi Arabia
[4]Department of Mathematics and Statistics, College of Science, Imam Mohammad Ibn Saud Islamic University (IMSIU), Riyadh, Saudi Arabia
Sayed011258@science.bsu.edu.eg, iodridi@uqu.edu.sa, aahmari@uqu.edu.sa, mmessaoudi@imamu.edu.sa

ARTICLE INFO

Article History:
Received: March 19, 2025
1st revised: April 20, 2025
2nd revised: April 24, 2025
Accepted: April 29, 2025
Published Online: May 20, 2025

Keywords:
Fractional calculus
Glucose-insulin model
Numerical methods
Chaos control
Numerical simulation
MSGDTM
JSCSM

AMS Classification:
46C05; 49J20; 93C20; 49K20; 34K05; 34A12; 26A33

ABSTRACT

This study applies the Multi-Step Generalized Differential Transform Method (MSGDTM) and the Jumarie-Stancu Collocation Series Method (JSCSM) to analyze a fractional-order Model (1). The model incorporates Caputo fractional derivatives to capture the nonlocal and memory-dependent characteristics of glucose-insulin interactions, considering physiological factors such as β-cell activity and external glucose intake. Stability analysis reveals bifurcations and chaotic attractors, demonstrating the system's sensitivity to fractional orders. Numerical simulations compare MSGDTM and JSCSM accuracy and efficiency, highlighting MSGDTM's superior convergence and lower approximation error. The results show that fractional-order modeling provides a more accurate framework for understanding glucose-insulin dynamics and predicting metabolic behavior. Furthermore, control mechanisms are introduced to mitigate chaos, offering potential strategies for managing diabetes. This work emphasizes the robustness of MSGDTM in solving complex fractional biological models. It provides insights into fractional calculus applications in biomedical research.

1. Introduction

Insulin regulation is a cornerstone of human metabolic processes, with imbalances leading to diabetes mellitus, a chronic condition affecting millions worldwide. Understanding the glucose-insulin interaction is crucial for developing effective treatment strategies. Traditional integer-order models are widely used to describe these interactions; however, they often fail to capture the complex physiological memory and hereditary properties inherent in biological systems. To address this limitation, fractional-order differential equations (FDEs) have emerged as a powerful tool, incorporating memory effects and nonlocal dynamics that better represent real-world biological phenomena.

Fractional calculus, characterized by its nonlocal operators and ability to retain memory

*Corresponding Author

effects, provides a flexible and robust mathematical framework for modeling intricate biological systems.[1,2] Its growing significance spans various disciplines, including engineering,[3] plant epidemiology,[4] mathematical biology,[5] medicine,[6] psychology, and life sciences.[7] Additionally, it finds applications in viscoelasticity,[8] electromagnetic wave propagation,[9] quantum mechanics,[10] physics,[11-22] and diabetes modeling,[23-34] Computer virus, zoonotic disease.[35] A key focus of this study is to analyze system stability, bifurcation structures, and chaotic dynamics using tools such as phase portraits, Lyapunov exponents, and bifurcation diagrams.[36,37]

In order to mitigate chaotic fluctuations, a simple linear controller is introduced. Studies show that fractional-order models enhance glucose-insulin interactions, leading to improved diabetes management strategies.[38–40] This research integrates fractional calculus, chaos theory, and computational simulations to advance both theoretical and applied aspects of glucose-insulin regulation, emphasizing memory effects in biological processes, and paving the way for biomedical progress. This work delves into the intricate behavior and regulatory mechanisms of the proposed model, leveraging memory-dependent fractional derivatives to capture long-term physiological interactions. Using advanced computational methods, including the MSGDTM and the JSCSM, the study formulates and analyzes a time-dependent fractional-order model of glucose-insulin dynamics, incorporating the interplay between glucose levels, insulin secretion, and beta-cell activity. These numerical schemes effectively solve the complex fractional differential equations governing the system's behavior.[41-65] Tsai and Chen[44] introduced the Laplace-Adomian-Padé approximation method, while Zeng et al.[45] derived analytical approximations for FDEs. Additionally, Khan et al.[46] combined the LADM in prior studies; see also.[44,45,47,48] Analytical techniques for solving fractional differential equations include the ADM,[49] the LADM,[50] the ADM,[51] the HAM,[52] the MSGDTM,[53] the Galerkin finite element method,[54] the Legendre wavelets method,[55] the spectral collocation method,[56] and JSCSM.[66] This study contributes an improved variant of the generalized differential transform method (GDTM),[57-60] refined to enhance solution accuracy over extended time intervals. Traditional GDTM approaches are limited to short-term approximations due to small time steps. By contrast, MSGDTM extends solution validity over longer periods while maintaining high precision, outperforming conventional techniques.[61-73] Numerical comparisons indicate strong agreement between the MSGDTM solutions and those obtained via the classical Runge-Kutta method when the derivative order is set to one.

It was proposed by Ackerman et al. (1964) that a 2D linear differential equation could be used to represent glucose tolerance test data. The mathematical model proposed is as follows:

$$\begin{aligned}\dot{\hat{u}}(\iota) &= \mathrm{a}_1\hat{v}(\iota) - \mathrm{a}_2\hat{u}(\iota) + c_1,\\ \dot{\hat{v}}(\iota) &= -\mathrm{a}_3\hat{v}(\iota) - \mathrm{a}_4\hat{u}(\iota) + c_2 + I.\end{aligned}$$

In these equations, $\hat{u}$ and $\hat{v}$ denote insulin and glucose concentrations, respectively, and I indicates the rate at which blood glucose levels increase. Based on the Lotka-Volterra framework (Elsadany et al.,[Elsadany] Shabestari et al.[75] developed a model to analyze glucose-insulin relationships. In this model:[75]

$$\begin{aligned}{}^{\mathrm{C}}\mathscr{D}^{\alpha}_{0,\iota}\hat{u}(\iota) =& -\mathrm{a}_1\hat{u}(\iota) + \mathrm{a}_2\hat{u}(\iota)\hat{v}(\iota) + \mathrm{a}_3\hat{v}^2(\iota) + \mathrm{a}_4\\ & \hat{v}^3(\iota) + \mathrm{a}_5\hat{w}(\iota) + \mathrm{a}_6\hat{w}^2(\iota) + \mathrm{a}_7\hat{w}^3(\iota)\\ & + \mathrm{a}_{20},\\ {}^{\mathrm{C}}\mathscr{D}^{\alpha}_{0,\iota}\hat{v}(\iota) =& -\mathrm{a}_8\hat{u}(\iota)\hat{v}(\iota) - \mathrm{a}_9\hat{u}^2(\iota) - \mathrm{a}_{10}\hat{u}^3(\iota)\\ & + \mathrm{a}_{11}\hat{v}(\iota)(1-\hat{v}(\iota)) - \mathrm{a}_{12}\hat{w}(\iota) - \mathrm{a}_{13}\\ & \hat{w}^2(\iota) - \mathrm{a}_{14}\hat{w}^3(\iota) + \mathrm{a}_{21},\\ {}^{\mathrm{C}}\mathscr{D}^{\alpha}_{0,\iota}\hat{w}(\iota) =& \mathrm{a}_{15}\hat{v}(\iota) + \mathrm{a}_{16}\hat{v}^2(\iota) + \mathrm{a}_{17}\hat{v}^3(\iota)\\ & - \mathrm{a}_{18}\hat{w}(\iota) - \mathrm{a}_{19}\hat{v}(\iota)\hat{w}(\iota).\end{aligned} \tag{1}$$

The model parameters are defined as follows: a_1 represents the natural decay rate of insulin in the absence of glucose, while a_2 quantifies the influence of glucose on insulin stimulation and a_3 captures the acceleration of insulin production as glucose levels rise. The basal secretion of insulin from β-cells, independent of glucose, is governed by a_4, with a_5 accounting for a minor contribution to basal insulin release and a_6 serving as an adjustment factor in basal insulin dynamics. Parameter a_7 introduces a positive feedback component to insulin release from β-cells. Insulin's regulatory effect on glucose metabolism is modeled by a_8, whereas a_9 and a_{10} represent strong and secondary reductions in glucose concentration due to insulin activity. The increase in glucose from external sources or metabolism without insulin influence is described by a_{11}. Parameters

a_{12}, a_{13}, and a_{14} characterize the effects of β-cell-derived insulin on lowering glucose levels, including both negative modulation and auxiliary impacts. The dynamics of β-cell growth and decline are detailed by a_{15}, which captures activation due to glucose elevation; a_{16}, which accounts for inhibitory influences at higher glucose levels; and a_{17}, a supporting factor for glucose-driven β-cell expansion. The natural loss of β-cells over time is modeled by a_{18}, while a_{19} reflects a progressive decline in β-cell population. Lastly, a_{20} represents a constant term for external input or loss in glucose dynamics. a_{21} denotes the baseline rate of insulin synthesis under normal physiological conditions. Glucose-insulin fractional order is given by

$$\begin{aligned}
{}^{\mathrm{C}}\mathscr{D}^{\alpha}_{0,\iota}\hat{u}(\iota) =& -\mathrm{a}_1\hat{u}(\iota) + \mathrm{a}_2\hat{u}(\iota)\hat{v}(\iota) + \mathrm{a}_3\hat{v}^2(\iota) \\
&+ \mathrm{a}_4\hat{v}^3(\iota) + \mathrm{a}_5\hat{w}(\iota) + \mathrm{a}_6\hat{w}^2(\iota) \\
&+ \mathrm{a}_7\hat{w}^3(\iota) + \mathrm{a}_{20} - d_1(\hat{v}+\hat{w}), \\
{}^{\mathrm{C}}\mathscr{D}^{\alpha}_{0,\iota}\hat{v}(\iota) =& -\mathrm{a}_8\hat{u}(\iota)\hat{v}(\iota) - \mathrm{a}_9\hat{u}^2(\iota) - \mathrm{a}_{10}\hat{u}^3(\iota) \\
&+ \mathrm{a}_{11}\hat{v}(\iota)(1-\hat{v}(\iota)) - \mathrm{a}_{12}\hat{w}(\iota) \\
&- \mathrm{a}_{13}\hat{w}^2(\iota) - \mathrm{a}_{14}\hat{w}^3(\iota) + \mathrm{a}_{21}, \\
{}^{\mathrm{C}}\mathscr{D}^{\alpha}_{0,\iota}\hat{w}(\iota) =& \mathrm{a}_{15}\hat{v}(\iota) + \mathrm{a}_{16}\hat{v}^2(\iota) \\
&+ \mathrm{a}_{17}\hat{v}^3(\iota) - \mathrm{a}_{18}\hat{w}(\iota) \\
&- \mathrm{a}_{19}\hat{v}(\iota)\hat{w}(\iota) - d_2(\hat{u}+\hat{v}+\hat{w}).
\end{aligned} \tag{2}$$

Using Caputo derivatives, this study proposes and examines a Model (1). It focuses on assessing system stability, bifurcation patterns, and chaotic dynamics across fractional orders. In addition, the research evaluates how well the MSGDTM and the JSCSM solve fractional differential equations, emphasizing their computational efficiency and accuracy. Moreover, the study explores effective control strategies to suppress chaotic fluctuations and enhance glucose stability.

The remainder of this paper is organized as follows. Section 2 discusses fractional calculus and the Caputo derivative. MSGDTM and JSCSM are applied to the glucose-insulin model in Section 3, along with a comparison. Numerical simulations, bifurcation analyses, and stability results are presented in Section 4. In Section 5, we summarize key findings and discuss potential future research directions in fractional-order biomedical modeling.

2. Stability investigation

Equation (1) has the following Jacobian matrix:

$$J(\hat{u},\hat{v},\hat{w}) = \begin{pmatrix} -a_s\hat{v} - 2a_g\hat{u} - 3a_{10}\hat{u}^2 \\ 0 \\ \\ -a_1 + a_2\hat{v} \\ -a_8\hat{u} + a_{11}(1-2\hat{v}) \\ a_{15} + 2a_{16}\hat{v}\_3a_{17}\hat{v}^2 - a_{19}\hat{w} \\ \\ a_2\hat{u} + 2a_3\hat{v} + 3a_4\hat{v} \\ -a_{12} - 2a_{13}\hat{w} - 3a_{14}\hat{w}^2 \\ -a_{18} - a_{19}\hat{v} \\ \\ a_5 + 2a_6\hat{w} + 3a_7\hat{w}^2 \end{pmatrix}$$

Following the approach in Shabestari et al. (2018), equilibrium points $E_1(0.805, 1.815, 1.319)$ and $E_2(0.624, 0.935, 0.877)$ are considered. The eigenvalues of system (1) at E_1 are $\Lambda_{1,2} = -1.7564 \pm 7.5090i$ and $\Lambda_3 = 1.3802$. For E_2, they are $\Lambda_{1,2} = 0.5262 \pm 2.3472i$ and $\Lambda_3 = -2.8372$. Define:

$$\Delta(\lambda) = \mathrm{diag}\left(\lambda^{M\alpha_1}, \lambda^{M\alpha_2}, \lambda^{M\alpha_3}\right) - J.$$

For linear systems to be asymptotically stable, the following must hold:

$$|\arg(\lambda)| > \frac{\pi}{2M}.$$

For instability at equilibrium points, the condition is:

$$\frac{\pi}{2M} - \min_j\{\arg(\Lambda_j)\} \geq 0,$$

where Λ_j are roots of $\det\left(\mathrm{diag}\left(\lambda^{Mq_x}, \lambda^{Mq_y}, \lambda^{Mq_z} - \boldsymbol{J}_{E_j}\right) = 0\right.$ for each equilibrium E_j $(i = 1, 2, 3)$.

$$\alpha < \frac{2}{\pi}\min_j|\arg(\Lambda_j)| \approx 0.86.$$

For chaotic attractors in the model (1), the following must be satisfied:

$$\frac{\pi}{2M} - \min_j\{|\arg(\Lambda_j)|\} \geq 0.$$

According to Table 1, the equilibrium points E_1 and E_2 behave as saddle points of index two.

Table 1 also presents the Kaplan-Yorke (KY) dimension for various fractional derivatives, computed as:

$$\dim(LE) = 2 + \frac{LE_1 + LE_2}{|LE_3|}.$$

Table 2 compares KY dimensions of different fractional derivatives, revealing that system (1)

possesses a relatively higher dimension of 2.09, indicating increased complexity.

3. Bifurcation diagrams

The parameter a_{16} could represent the system's response to stress or external factors affecting glucose regulation. a_{16} (-2 to 0) could represent the system's response to stress or external factors affecting glucose regulation. Bifurcations may indicate shifting glucose levels due to changing external conditions. Related dynamics is bifurcation in a_{16} shows external stressors affect glucose dynamics. In a bifurcated liver, a parameter a_{17} could describe the delay in insulin response, with bifurcations representing an oscillatory glucose response. a_{17} (0 to 1) may describe insulin response delay. As response times vary, bifurcations may indicate changes from stable glucose regulation to oscillatory or chaotic behavior. The bifurcation in a_{17} might be related to liver response delays. Insulin and other metabolic pathways might be represented by a_{18}. There might be interactions between insulin and other metabolic pathways in a_{18}. a_{18} bifurcations (-1 to 0) may indicate a change from stable to complex glucose dynamics. A bifurcation in a_{18} may give insight into glucose regulation. An indicator of insulin resistance might be a_{19}. There is a possibility that the rate at which insulin resistance develops can be represented by a_{19} (-1 to 0). The point of bifurcation could result in a transition from stable glucose regulation to instability as resistance increases as the point of bifurcation is reached. In the case of an increase in a_{19}, this could be a result of varying rates at which insulin resistance develops as a result of variable insulin resistance levels leading to a change in glucose stability. In the system (1), there might be a parameter called a_{20} that describes the strength of feedback mechanisms that exist. It might be possible to describe the strength of feedback mechanisms in the Model (1) by the parameter a_{20}. It is possible that bifurcations in a_{20} (-1 to 0) could indicate that glucose dynamics are changing from stable to complex due to changes in the strength of feedback. This could be attributed to the bifurcation of a_{20} indicating how variations in feedback strength can affect the stability of glucose levels. A parameter known as a_{21} is used as a potential indicator of how multi-factor influences glucose regulation in a system. In order to better understand how several factors act on the regulation of glucose, a_{21} (-1 to 0) might be a good indicator. Bifurcations could indicate transitions from stable to chaotic behavior as these factors vary. It is possible that the bifurcation in a_{21} could be a reflection of multiple influences that combine to affect glucose dynamics and stability overall. During the regulation of glucose and insulin dynamics within the human body, every parameter from a_1 to a_{21} is crucial. Diabetes requires understanding these bifurcations to predict and manage the complex dynamics of glucose regulation. Predicting and controlling critical transitions in complex systems, whether biological or physical, requires understanding bifurcation. Stability may shift to chaos or vice versa, affecting the stability and behavior of the system. By understanding these bifurcations, we can develop strategies for managing biological processes, designing stable physical systems, and preventing undesirable behaviors. Critical transitions can be predicted and controlled by understanding the bifurcation of parameters in complex systems. During these transitions, the system can go from stability to chaos or vice versa, affecting its behavior and stability significantly. By recognizing these bifurcations, we can design stable physical systems and prevent undesirable behaviors like chaotic oscillations.

4. Methods

4.1. Jumarie-Stancu collocation series method

We apply the JSCSM to approximate the solutions for $\hat{u}(t)$, $\hat{v}(t)$, and $\hat{w}(t)$ in the following steps.

Assume each function can be expanded as a series:

$$\hat{u}(t) = \Sigma_{n=0}^{\infty} a_n \iota^n,$$
$$\hat{v}(t) = \Sigma_{n=0}^{\infty} b_n \iota^n,$$
$$\hat{w}(t) = \Sigma_{n=0}^{\infty} c_n \iota^n,$$

where a_n, b_n, and c_n are coefficients to be determined for $\hat{u}$, $\hat{v}$, and $\hat{w}$, respectively.

Using the Jumarie fractional derivative, we approximate the fractional Caputo derivative ${}^{\mathtt{C}}\mathscr{D}_{0,\iota}^{\alpha}$ for each series term:

$${}^{\mathtt{C}}\mathscr{D}_{0,\iota}^{\alpha} \iota^n \approx \frac{\iota^{n-\alpha}}{\alpha(n+1)} \cdot \alpha(n+1-\alpha).$$

Then, each derivative can be represented as:

$${}^{\mathtt{C}}\mathscr{D}_{0,\iota}^{\alpha} \hat{u}(t) \approx \Sigma_{n=0}^{\infty} a_n \, {}^{\mathtt{C}}\mathscr{D}_{0,\iota}^{\alpha}(\iota^n),$$
$${}^{\mathtt{C}}\mathscr{D}_{0,\iota}^{\alpha} \hat{v}(t) \approx \Sigma_{n=0}^{\infty} b_n \, {}^{\mathtt{C}}\mathscr{D}_{0,\iota}^{\alpha}(\iota^n),$$
$${}^{\mathtt{C}}\mathscr{D}_{0,\iota}^{\alpha} \hat{w}(t) \approx \Sigma_{n=0}^{\infty} c_n \, {}^{\mathtt{C}}\mathscr{D}_{0,\iota}^{\alpha}(\iota^n).$$

Select collocation points $\{\iota_0, \iota_1, \ldots, \iota_m\}$ within the time interval of interest.

Substitute the series and fractional derivative approximations into each of the differential equations:

$$\Sigma_{n=0}^{\infty} a_n {}^{\mathtt{C}}\mathscr{D}_{0,\iota}^{\alpha}(\iota_j^n) = -a_1\hat{u}(\iota_j) + a_2\hat{u}(\iota_j)\hat{v}(\iota_j) + \cdots + a_{20},$$
$$\Sigma_{n=0}^{\infty} b_n {}^{\mathtt{C}}\mathscr{D}_{0,\iota}^{\alpha}(\iota_j^n) = -a_8\hat{u}(\iota_j)\hat{v}(\iota_j) - \cdots + a_{21},$$
$$\Sigma_{n=0}^{\infty} c_n {}^{\mathtt{C}}\mathscr{D}_{0,\iota}^{\alpha}(\iota_j^n) = a_{15}\hat{v}(\iota_j) + \cdots - a_{19}\hat{v}(\iota_j)\hat{w}(\iota_j),$$

where $j = 0, 1, \ldots, m$.

Based on the complexity of the algebraic system, the coefficients a_n, b_n, and c_n can be determined numerically or symbolically. Once the coefficients are determined, approximate solutions are constructed as:

$$\hat{u}(t) \approx \Sigma_{n=0}^{N} a_n \iota^n,$$
$$\hat{v}(t) \approx \Sigma_{n=0}^{N} b_n \iota^n,$$
$$\hat{w}(t) \approx \Sigma_{n=0}^{N} c_n \iota^n,$$

where N is the number of terms chosen based on the desired accuracy.

4.2. MSGDTM

Let the differential transforms of $\hat{u}(t)$, $\hat{v}(t)$, and $\hat{w}(t)$ be represented as $\hat{u}(\hat{k})$, $\hat{v}(\hat{k})$, and $\hat{w}(\hat{k})$, respectively. Assume the initial values satisfy $\hat{u}(0) = \hat{u}_0$, $\hat{v}(0) = \hat{v}_0$, and $\hat{w}(0) = \hat{w}_0$. The solution process begins with these initial conditions in the transformed domain at $k = 0$. Applying the recurrence relations derived earlier, we iteratively compute $\hat{u}(\hat{k}+1)$, $\hat{v}(\hat{k}+1)$, and $\hat{w}(\hat{k}+1)$ for each k up to the desired approximation order K. The approximate solutions in the original domain for $\hat{u}(t)$, $\hat{v}(t)$, and $\hat{w}(t)$ can then be reconstructed via the inverse differential transform. Using the MSGDTM methodology, partition the interval $[0, T]$ into M subintervals. To illustrate the approach, consider the system analyzed in:[63]-[67]

$$\begin{aligned}
\mathscr{D}_1^{\alpha} \upsilon_1(t) &= g_1(t, \upsilon_1, \upsilon_2, ..., \upsilon_n),\\
\mathscr{D}_2^{\alpha} \upsilon_2(t) &= g_2(t, \upsilon_1, \upsilon_2, ..., \upsilon_n),\\
&\vdots\\
\mathscr{D}_n^{\alpha} \upsilon_n(t) &= g_n(t, \upsilon_1, \upsilon_2, ..., \upsilon_n).
\end{aligned} \tag{3}$$

subject to

$$\upsilon_j(\iota_0) = d_j, \qquad i = 1, 2, ..., n, \tag{4}$$

The solution of the problem (3)-(4) is sought over the domain $[\iota_0, T]$. The kth-order approximation of the solution to this problem is:

$$\upsilon_j(t) = \sum_{j=0}^{K} \Gamma_j(\hat{k})(t - \iota_0)^{k\alpha_j}, \quad \iota \in [\iota_0, T],$$

where $\Gamma_j(\hat{k})$ satisfies

$$\frac{\alpha((\hat{k}+1)\alpha_j + 1)}{\alpha(k\alpha_j + 1)} \Gamma_j(\hat{k}+1) = g_j(k, \Gamma_1, \Gamma_2, ..., \Gamma_n),$$

and with initial conditions $\Gamma_j(0) = d_j$. The differential transform of $g_j(k, \Gamma_1, \Gamma_2, ..., \Gamma_n)$ corresponds to $g_j(t, \upsilon_1, \upsilon_2, ..., \upsilon_n)$ for $j = 1, 2, ..., n$. Partition the interval $[\iota_0, T]$ into M subintervals $[\iota_{m-1}, \iota_m]$, where $m = 1, 2, ..., M$, using a step size of $h = (T - \iota_0)/M$ and nodes $\iota_m = \iota_0 + mh$. The principles of MSGDTM are outlined below.

Initially, the MSGDTM method solves (3)-(4) on the first interval $[\iota_0, \iota_1]$, yielding the approximate solution $\upsilon_{i,1}(t)$ for $t \in [\iota_0, \iota_1]$. For $m \geq 2$, applying MSGDTM to (3)-(4) on $[\iota_{m-1}, \iota_m]$ uses the continuity condition $\upsilon_{i,m}(\iota_{m-1}) = \upsilon_{i,m-1}(\iota_{m-1})$. Repeating this process results in approximations $\upsilon_{i,m}(t)$ for all $m = 1, 2, ..., M$. The final approximation is defined as:

$$\upsilon_j(t) = \begin{cases} \upsilon_{i,1}(t) & \text{if } \iota \in [\iota_0, \iota_1],\\ \upsilon_{i,2}(t) & \text{if } \iota \in [\iota_1, \iota_2],\\ \vdots & \\ \upsilon_{i,M}(t) & \text{if } \iota \in [\iota_{M-1}, \iota_M]. \end{cases}$$

MSGDTM remains effective for all step sizes h. For system (1), the MSGDTM procedure yields:

$$\begin{aligned}
\hat{u}(\hat{k}+1) =& \frac{\alpha(\alpha k + 1)}{\alpha(\alpha(\hat{k}+1) + 1)} \Big(- b_1\hat{u}(\hat{k}) + b_2\hat{u}(\hat{k})\hat{v}(\hat{k}) + b_3\hat{v}^2(\hat{k})\\
&+ b_4\hat{v}^3(\hat{k}) + b_5\hat{w}(\hat{k}) + b_6\hat{w}^2(\hat{k})\\
&+ b_7\hat{w}^3(\hat{k}) + b_{20}\Big),\\
\hat{v}(\hat{k}+1) =& \frac{\alpha(\alpha k + 1)}{\alpha(\alpha(\hat{k}+1) + 1)} \Big(- b_8\hat{u}(\hat{k})\hat{v}(\hat{k}) - b_9\hat{u}^2(\hat{k}) - b_{10}\hat{u}^3(\hat{k})\\
&+ b_{11}\hat{v}(\hat{k})(1 - \hat{v}(\hat{k})) - b_{12}\hat{w}(\hat{k})\\
&- b_{13}\hat{w}^2(\hat{k}) - b_{14}\hat{w}^3(\hat{k}) + b_{21}\Big),\\
\hat{w}(\hat{k}+1) =& \frac{\alpha(\alpha k + 1)}{\alpha(\alpha(\hat{k}+1) + 1)} \Big(b_{15}\hat{v}(\hat{k}) + b_{16}\hat{v}^2(\hat{k}) + b_{17}\hat{v}^3(\hat{k})\\
&- b_{18}\hat{w}(\hat{k}) - b_{19}\hat{v}(\hat{k})\hat{w}(\hat{k})\Big).
\end{aligned}$$

The initial values: $\hat{u}(0) = d_1$, $\hat{v}(0) = d_2$, and $\hat{w}(0) = d_3$. Following is the differential transform

Table 1. Equilibrium points and their Eigenvalues

Equilibrium point and Eigenvalues	
$E_1(0.805, 1.815, 1.319)$	$\Lambda_{1,2} = -1.7564 \pm 7.5090i$, $\Lambda_3 = 1.3802$
$E_2(0.624, 0.935, 0.877)$	$\Lambda_{1,2} = 0.5262 \pm 2.3472i$, $\Lambda_3 = -2.8372$

Table 2. Lyapunov Exponents vs. α for Model (1)

α	LE1	LE2	LE3	dim(LE)
0.7	0.0182	-0.8429	-7.3948	1.88847
0.8	0.4326	-0.0034	-5.3810	2.079762
0.9	0.1163	-0.0685	-3.0441	2.01570
0.95	0.0529	-0.1489	-2.2316	1.956981
1.0	0.2045	-0.0038	-2.0108	2.099811

Table 3. Revised set of parameter values employed in this research, adapted from the model by Shabestari et al. [75]

a_1	2.04	a_2	0.10	a_3	1.09	a_4	-1.08
a_5	0.03	a_6	-0.06	a_7	2.01	a_8	0.22
a_9	-3.84	a_{10}	-1.20	a_{11}	0.30	a_{12}	1.37
a_{13}	-0.30	a_{14}	0.22	a_{15}	0.30	a_{16}	-1.35
a_{17}	0.50	a_{18}	-0.42	a_{19}	-0.15	a_{20}	-0.19
a_{21}	-0.56						

series solution for system (1):

$$\hat{u}(t) \simeq \sum_{k=0}^{K} \hat{U}(\hat{k})\iota^{\alpha k},$$
$$\hat{v}(t) \simeq \sum_{k=0}^{K} \hat{V}(\hat{k})\iota^{\alpha k},$$
$$\hat{w}(t) \simeq \sum_{k=0}^{K} \hat{W}(\hat{k})\iota^{\alpha k}.$$

For the MSGDTM approach, the series solution of system (1) is obtained similarly for $\hat{u}(t)$, $\hat{v}(t)$, and $\hat{w}(t)$.

4.3. MSGDTM and JSCSM error analysis

The approximation errors of the JSCSM and the MSGDTM when applied to the fractional glucose-insulin model are discussed here. The error is computed as the L_2-norm for the difference between the approximate solutions and a reference solution obtained using a high-accuracy numerical method.

For a given solution component $\hat{u}(t)$, the L_2-norm of the error is defined as:

$$\text{Error}(\hat{u}) = \sqrt{\frac{1}{M}\Sigma_{j=1}^{M}\big(\hat{u}_{\text{approx}}(\iota_j) - \hat{u}_{\text{ref}}(\iota_j)\big)^2},$$

where M is the total number of time points in the interval $[0, T]$, and $\hat{u}_{\text{approx}}(\iota_j)$ and $\hat{u}_{\text{ref}}(\iota_j)$ denote the approximate and reference solutions for the time point ι_j.

Similarly, the errors for $\hat{v}(t)$ and $\hat{w}(t)$ are defined. The total error is then given as:

$$\text{Total Error} = \sqrt{\text{Error}(\hat{u})^2 + \text{Error}(\hat{v})^2} + \sqrt{\text{Error}}(\hat{w})^2.$$

The procedure for error evaluation is the following:

(1) Compute $\hat{u}_{\text{JSCSM}}(t)$, $\hat{v}_{\text{JSCSM}}(t)$, and $\hat{w}_{\text{JSCSM}}(t)$ using JSCSM for a given truncation order N.
(2) Compute $\hat{u}_{\text{MSGDTM}}(t)$, $\hat{v}_{\text{MSGDTM}}(t)$, and $\hat{w}_{\text{MSGDTM}}(t)$ using MSGDTM for the same truncation order N.
(3) Compare both approximate solutions with a high-accuracy reference solution, $\hat{u}_{\text{ref}}(t)$, $\hat{v}_{\text{ref}}(t)$, and $\hat{w}_{\text{ref}}(t)$, obtained using a reliable numerical method such as the fractional Runge-Kutta method.
(4) Compute the L_2-norm for both methods.

The approximation errors for JSCSM and MSGDTM are compared across different truncation orders ($N = 5, 10, 15$) in Table 4. The table highlights the superiority of MSGDTM in achieving lower errors for the same truncation order.

From Table 4, it is evident the following:

- Both JSCSM and MSGDTM achieve higher accuracy as the truncation order N increases.
- MSGDTM consistently outperforms JSCSM in terms of approximation accuracy, achieving lower errors for all truncation orders tested.

Table 4. Approximation errors for JSCSM and MSGDTM at different truncation orders

Truncation Order (N)	Error (JSCSM)	Error (MSGDTM)
5	3.21×10^{-2}	2.11×10^{-2}
10	1.47×10^{-2}	8.95×10^{-3}
15	7.63×10^{-3}	4.02×10^{-3}

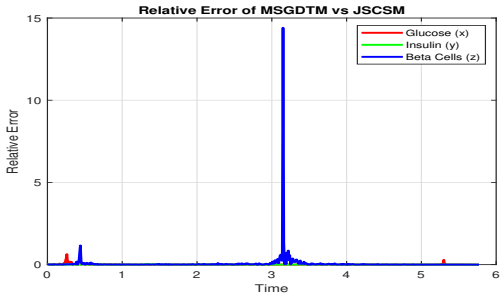

(g) Relative error of MSGDTM.

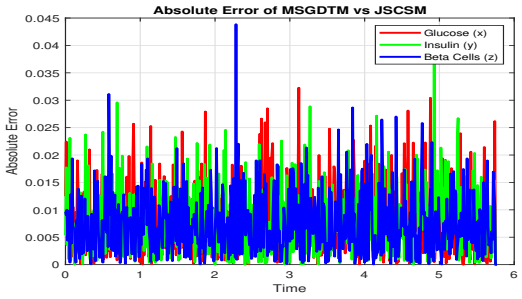

(h) Relative error of JSCSM

Figure 1. Relative error of MSGDTM versus JSCSM

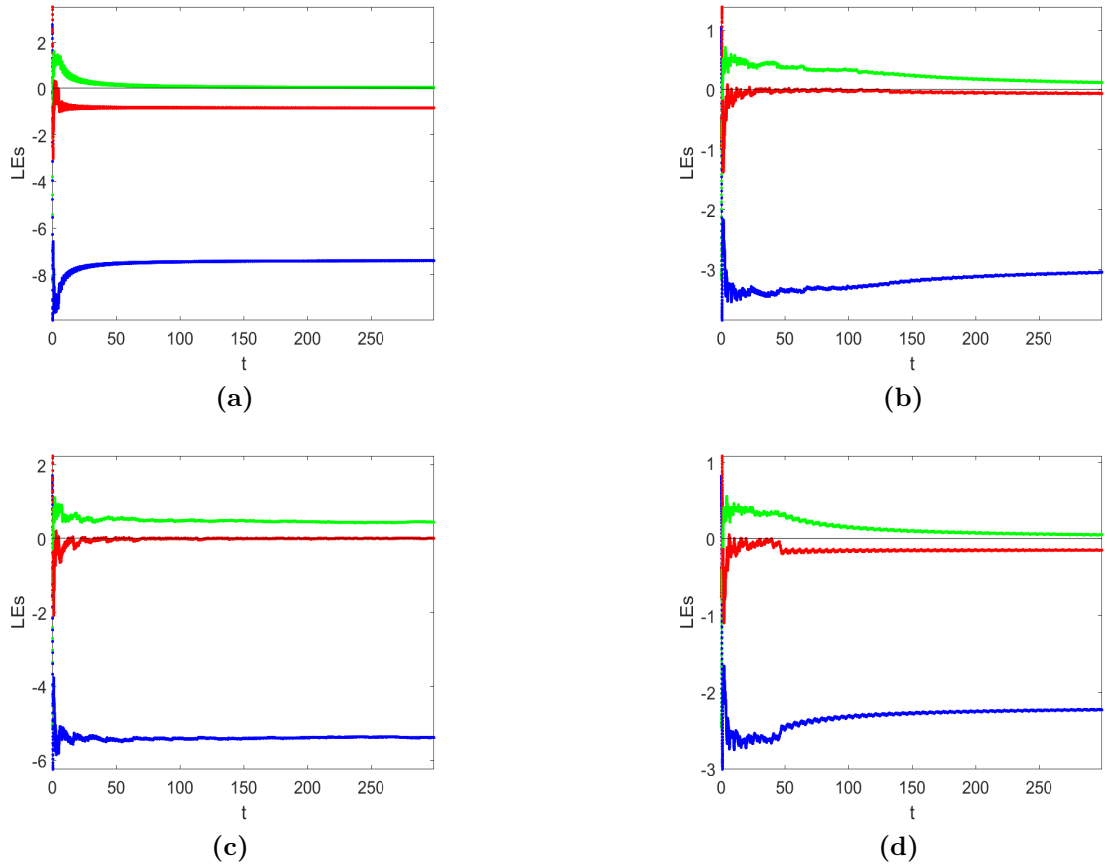

(a) **(b)** **(c)** **(d)**

Figure 2. Lyapunov exponents for Model (1)

- The faster convergence of MSGDTM can be attributed to its efficient handling of fractional dynamics over subintervals.

This analysis demonstrates the effectiveness of both methods in solving fractional-order systems. While MSGDTM offers superior accuracy, JSCSM remains a computationally viable approach for moderate truncation orders.

5. Model simulation and control analysis

This section presents graphical representations of the Model (1) under varying fractional orders and control implementations. Figures 5 and 6 display the temporal progression of glucose ($\hat{u}$), insulin ($\hat{v}$), and beta-cell function ($\hat{w}$) for both

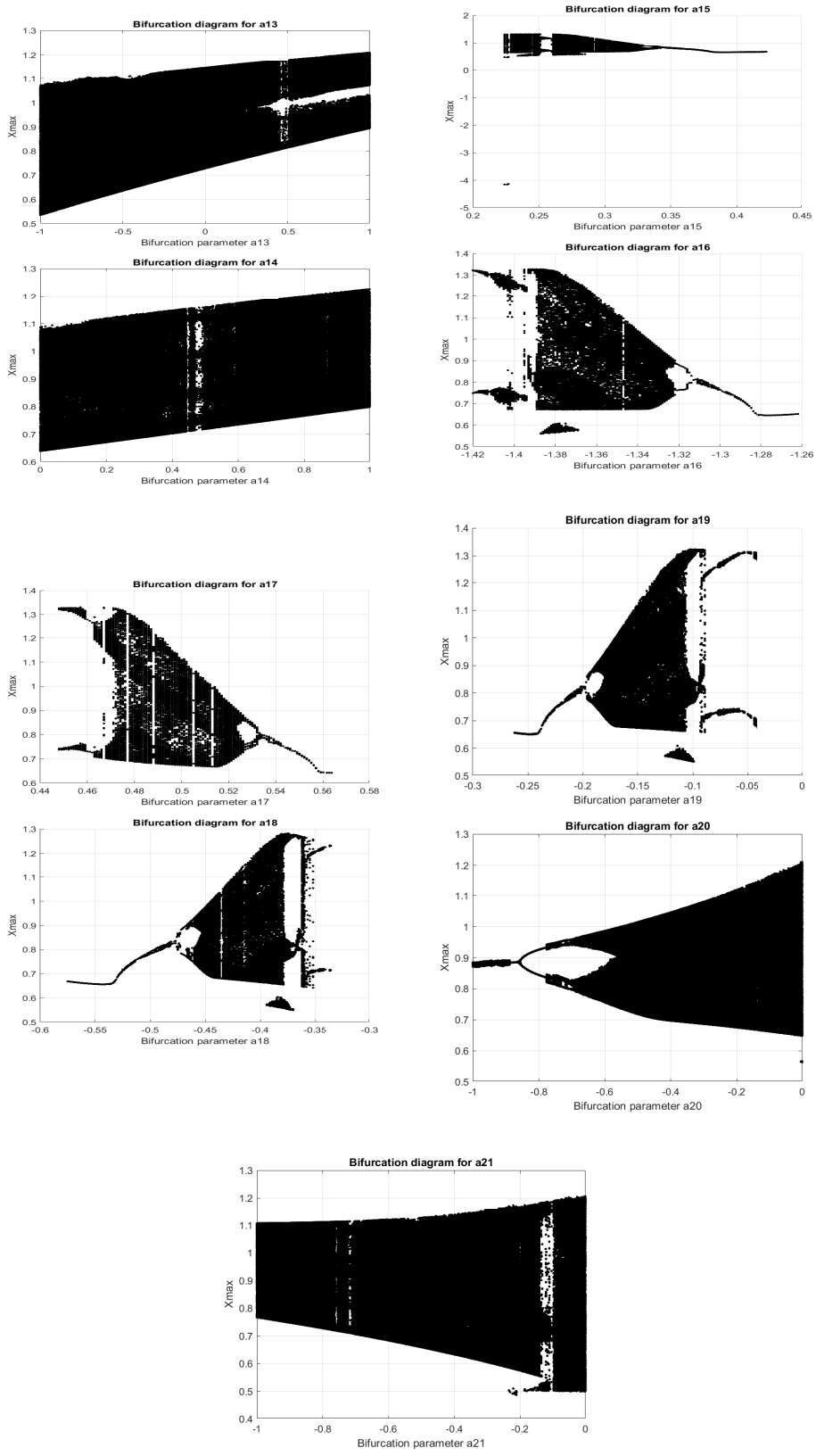

Figure 3. Model bifurcation (1)

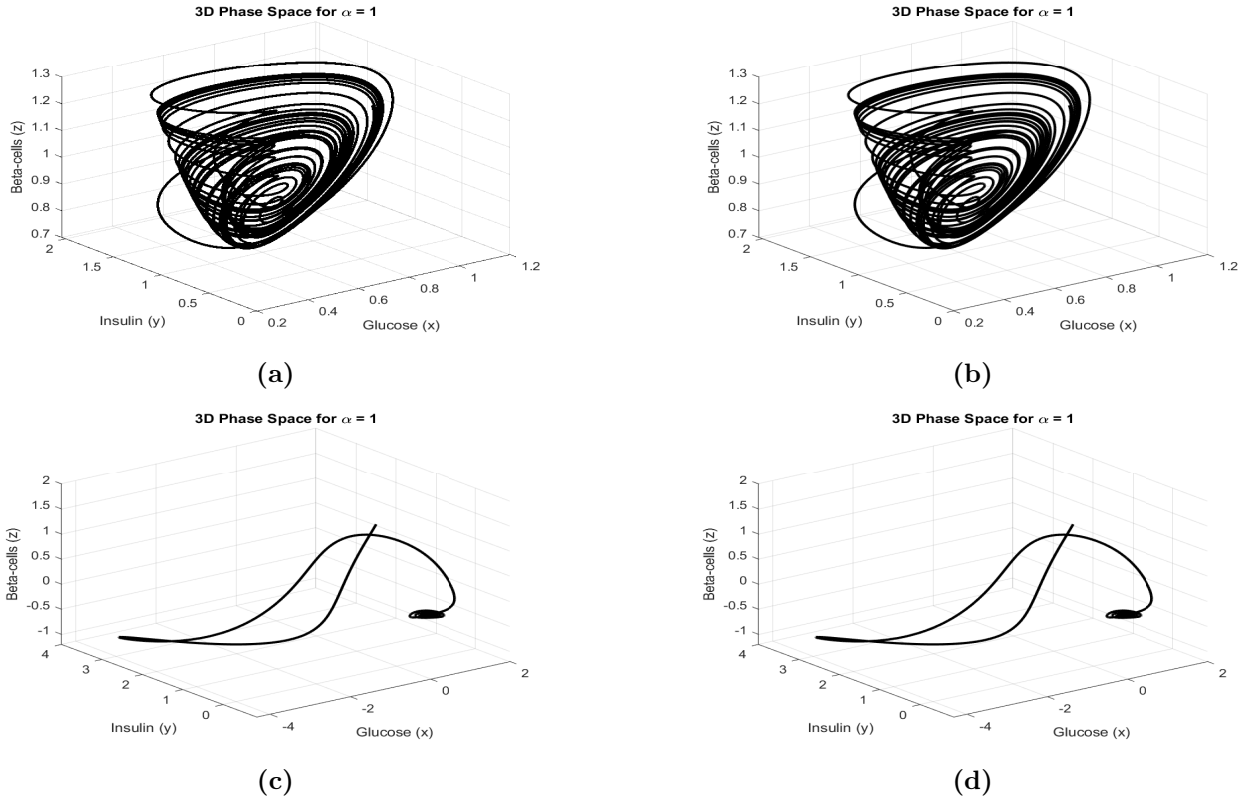

Figure 4. Compared between the 3D phases of (1) illustrated in (a), (b) and the controlled system (2) illustrated in (c), (d) under JSCSM and MSGDTM for $\alpha = 1$

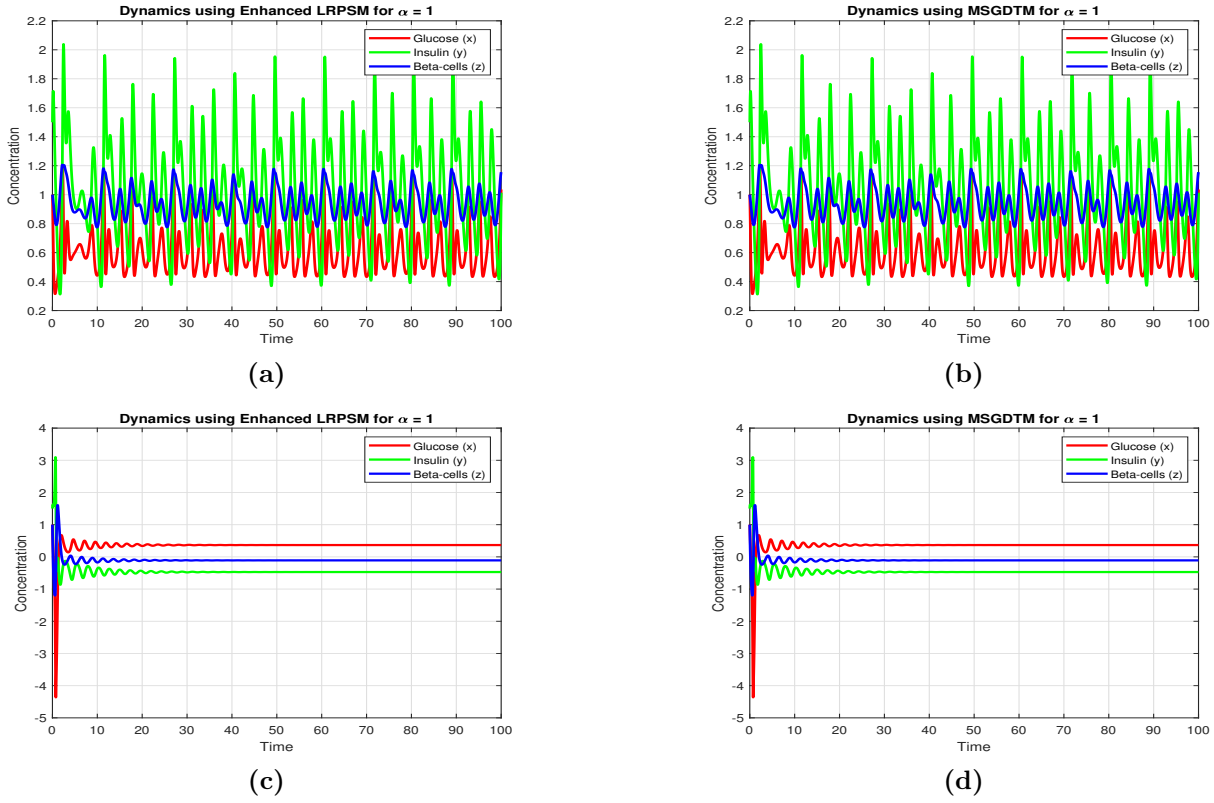

Figure 5. The time series of (1) shown in (a), (b) and the controlled system (2) shown in (c), (d) for $\alpha = 0.98$ under JSCSM and MSGDTM

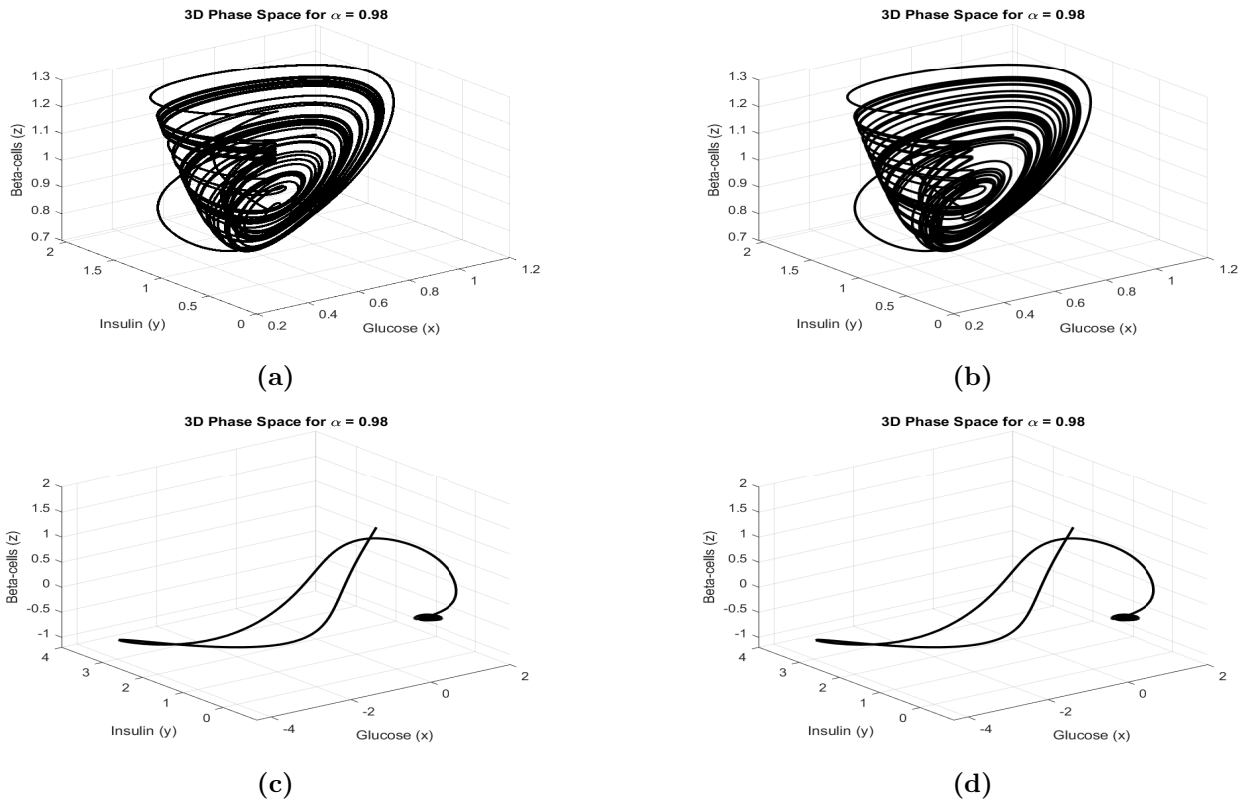

Figure 6. Compared between the 3D phases of (1) illustrated in (a), (b) and the controlled system (2) illustrated in (c), (d) under JSCSM and MSGDTM for $\alpha = 0.98$

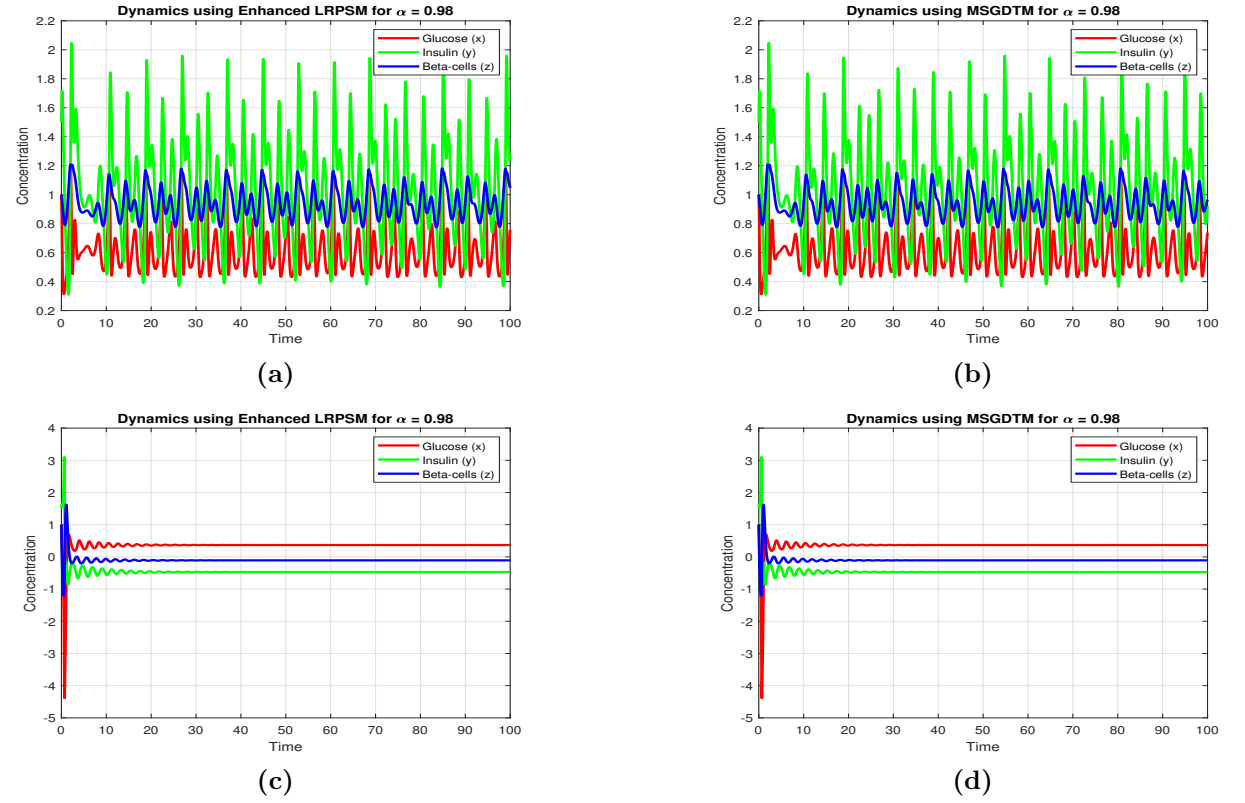

Figure 7. The time series of (1) shown in (a), (b) and the controlled system (2) shown in (c), (d) for $\alpha = 1$ under JSCSM and MSGDTM

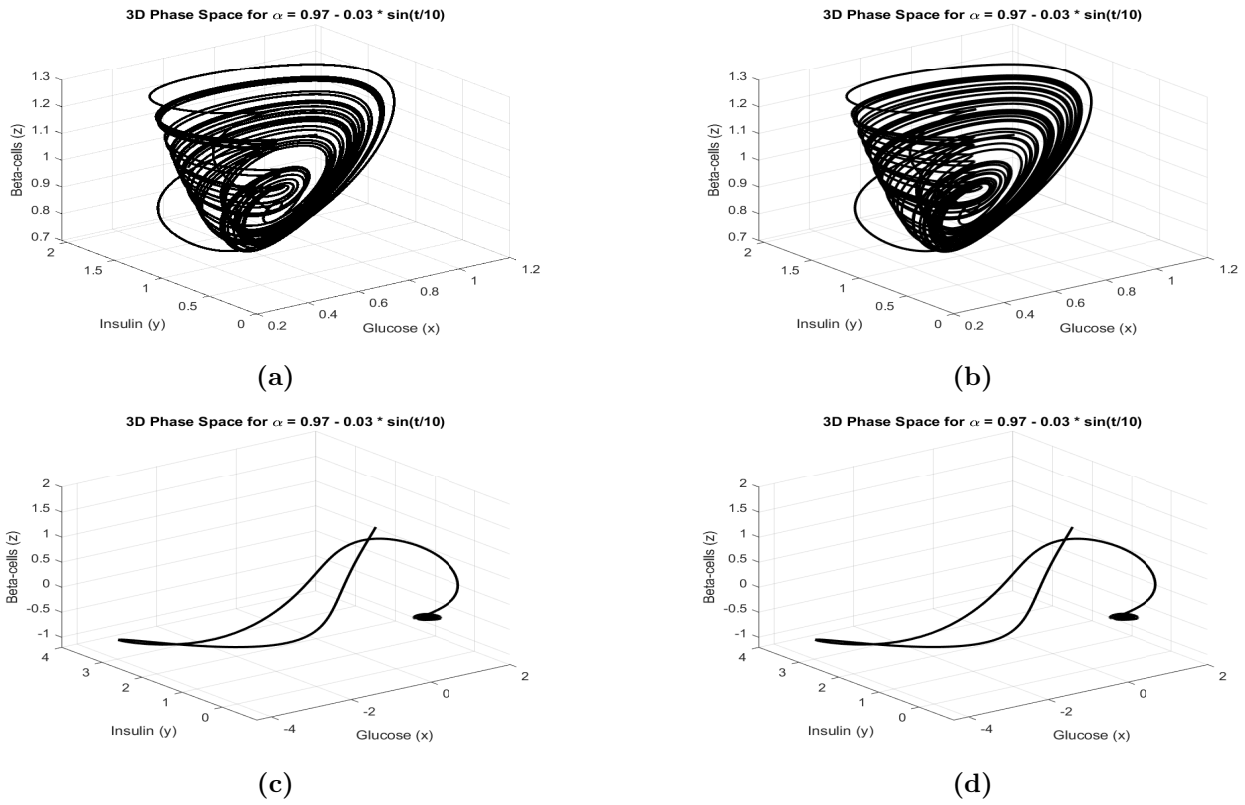

Figure 8. Compared between the 3D phases of (1) illustrated in (a), (b) and the controlled system (2) illustrated in (c), (d) under JSCSM and MSGDTM for $\alpha = 0.97 - 0.03 \times sin(t/10)$

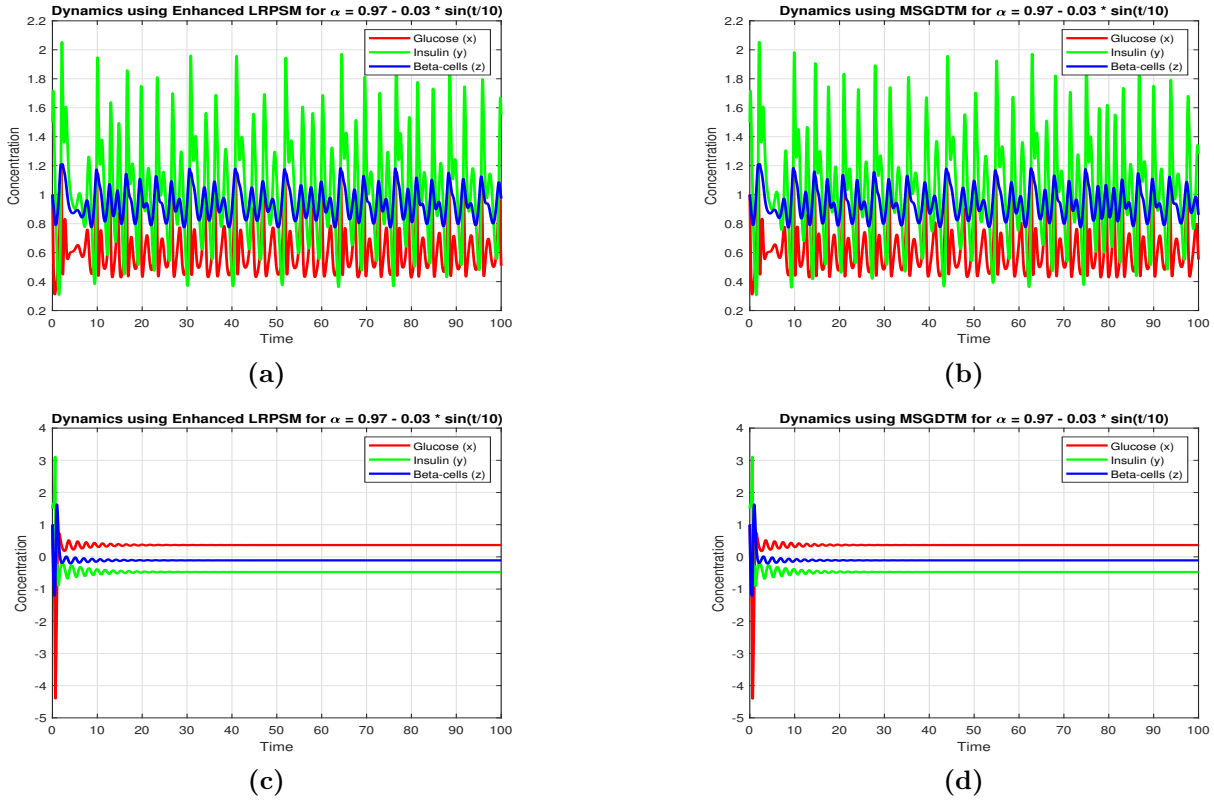

Figure 9. The time series of (1) shown in (a), (b) and the controlled system (2) shown in (c), (d) for $\alpha = 0.97 - 0.03 \times sin(t/10)$ under JSCSM and MSGDTM

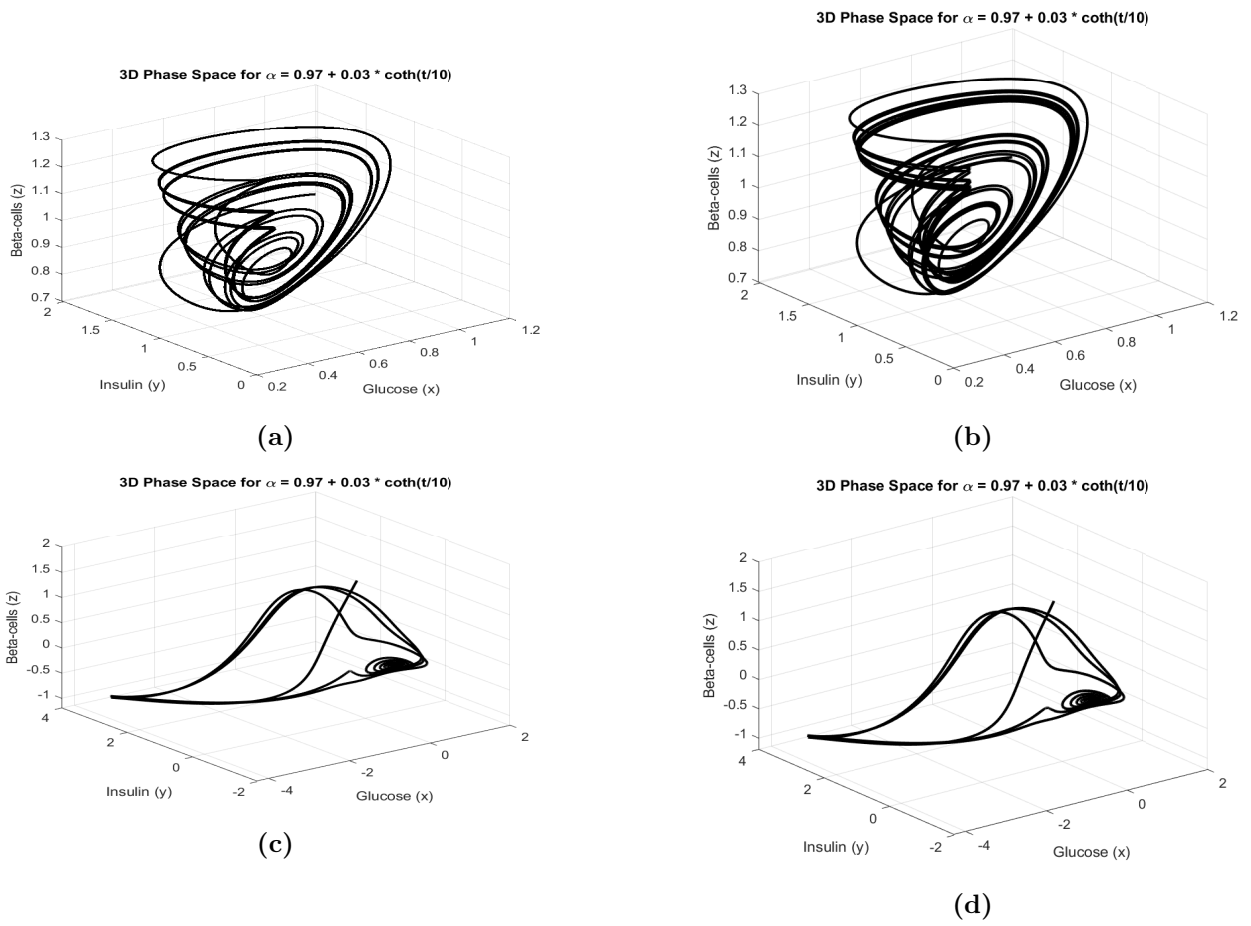

Figure 10. Compared between the 3D phases of (1) illustrated in (a), (b) and the controlled system (2) illustrated in (c), (d) under JSCSM and MSGDTM for $\alpha = 0.97 + 0.03 \times coth(t/10)$

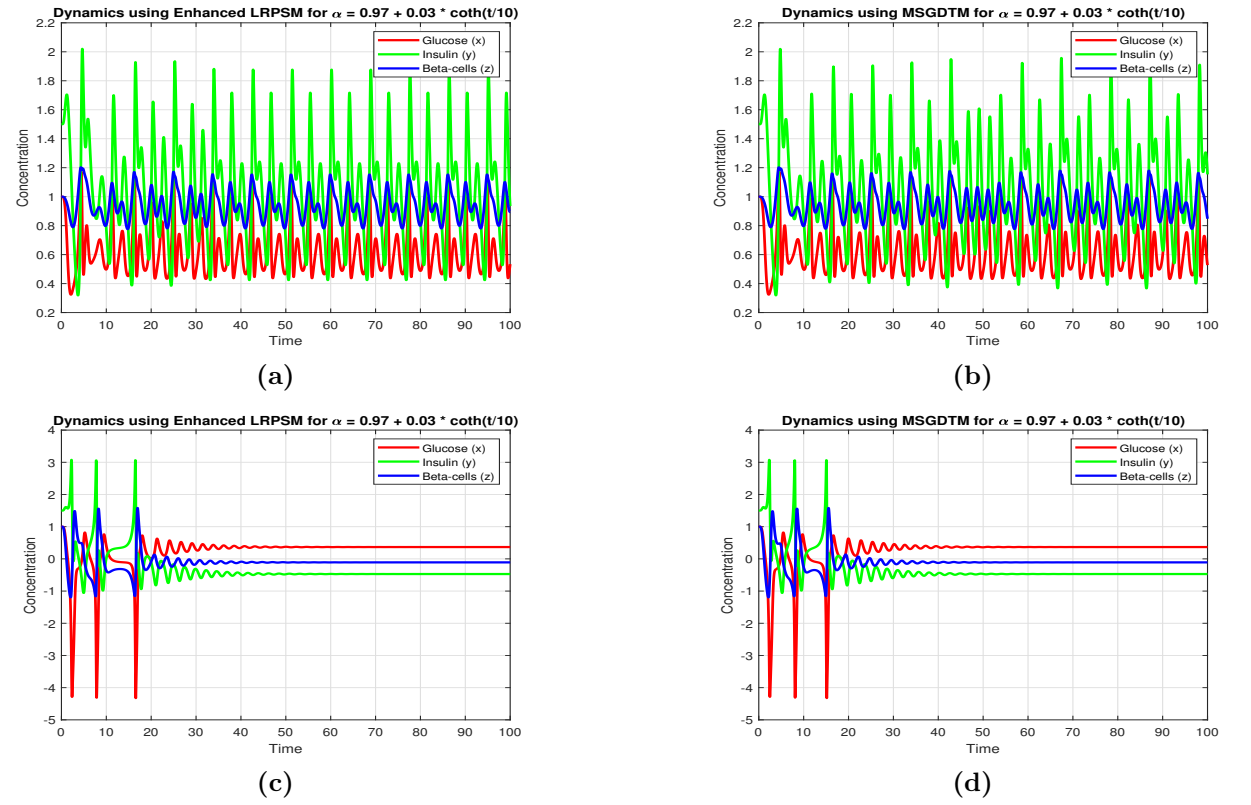

Figure 11. The time series of (1) shown in (a), (b) and the controlled system (2) shown in (c), (d) for $\alpha = 0.97 + 0.03 \times coth(t/10)$ under JSCSM and MSGDTM

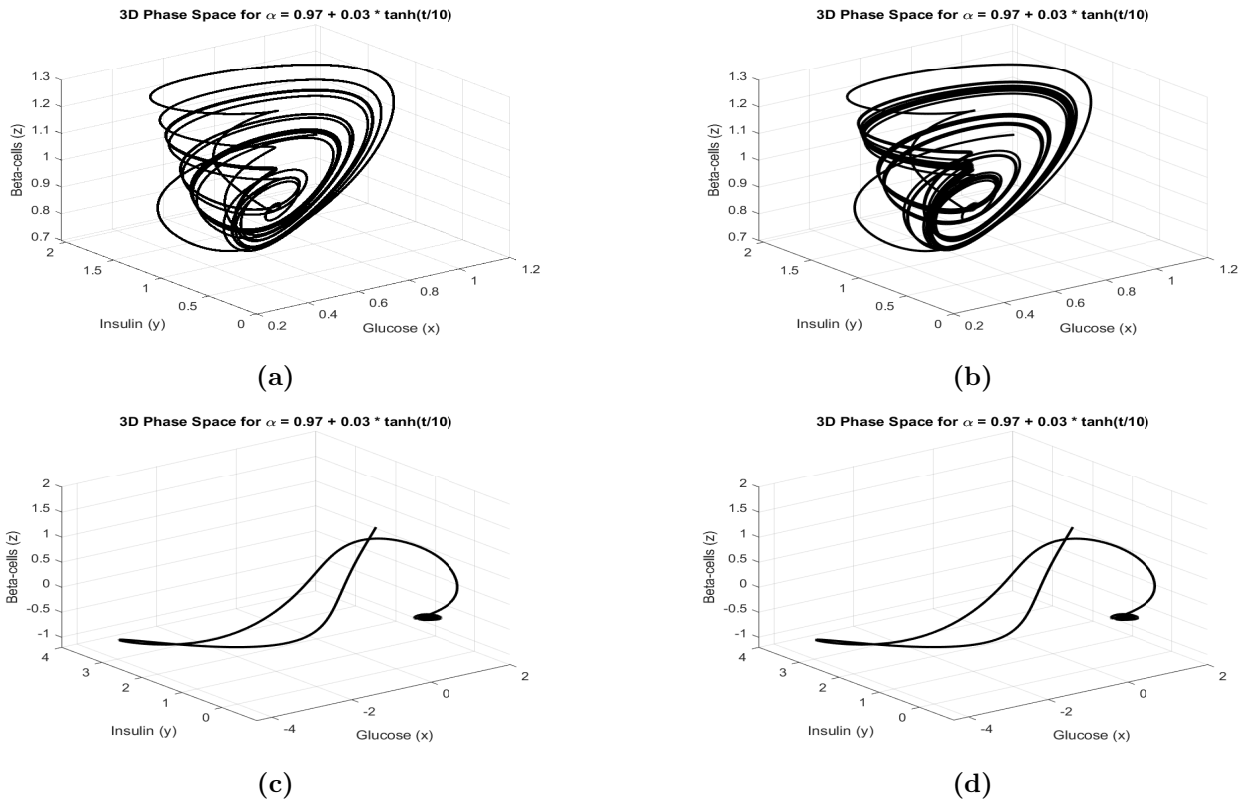

Figure 12. Compared between the 3D phases of (1) illustrated in (a), (b) and the controlled system (2) illustrated in (c), (d) under JSCSM and MSGDTM for $\alpha = 0.97 + 0.03 \times \tanh(t/10)$

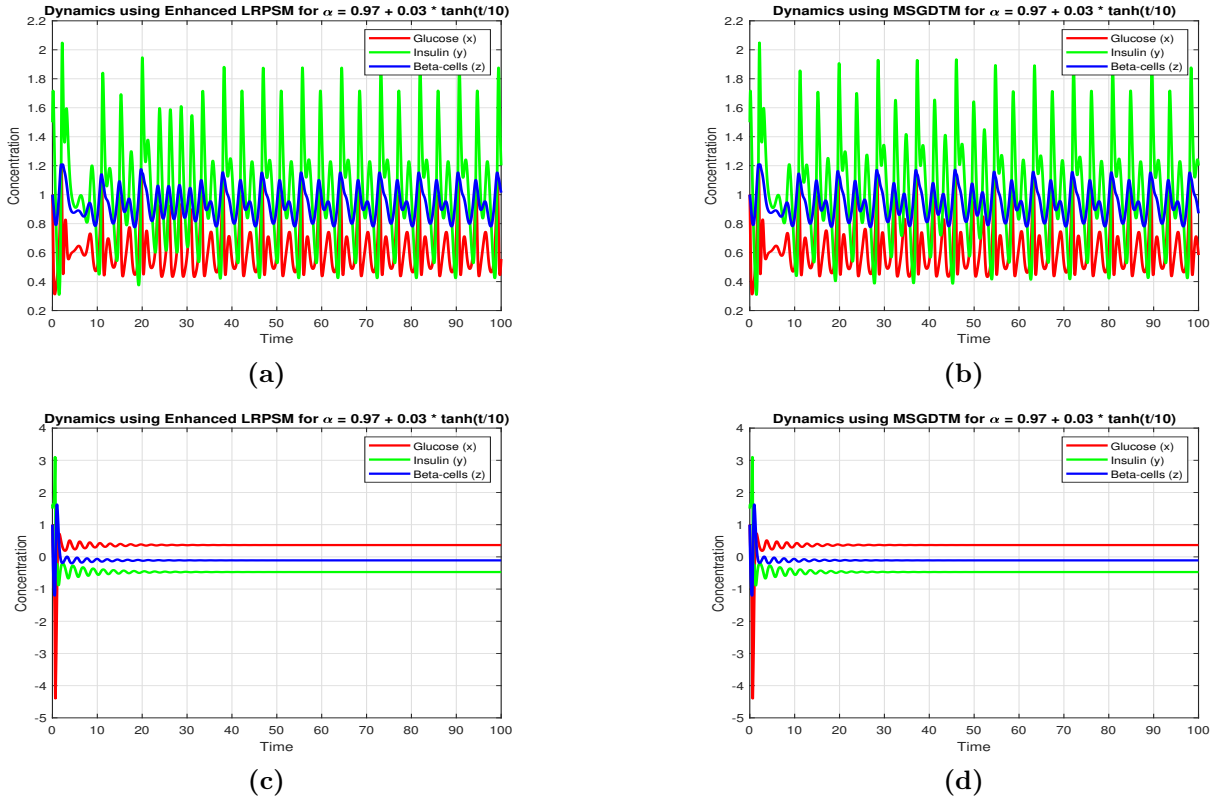

Figure 13. The time series of (1) shown in (a), (b) and the controlled system (2) shown in (c), (d) for $\alpha = 0.97 + 0.03 \times \tanh(t/10)$ under JSCSM and MSGDTM

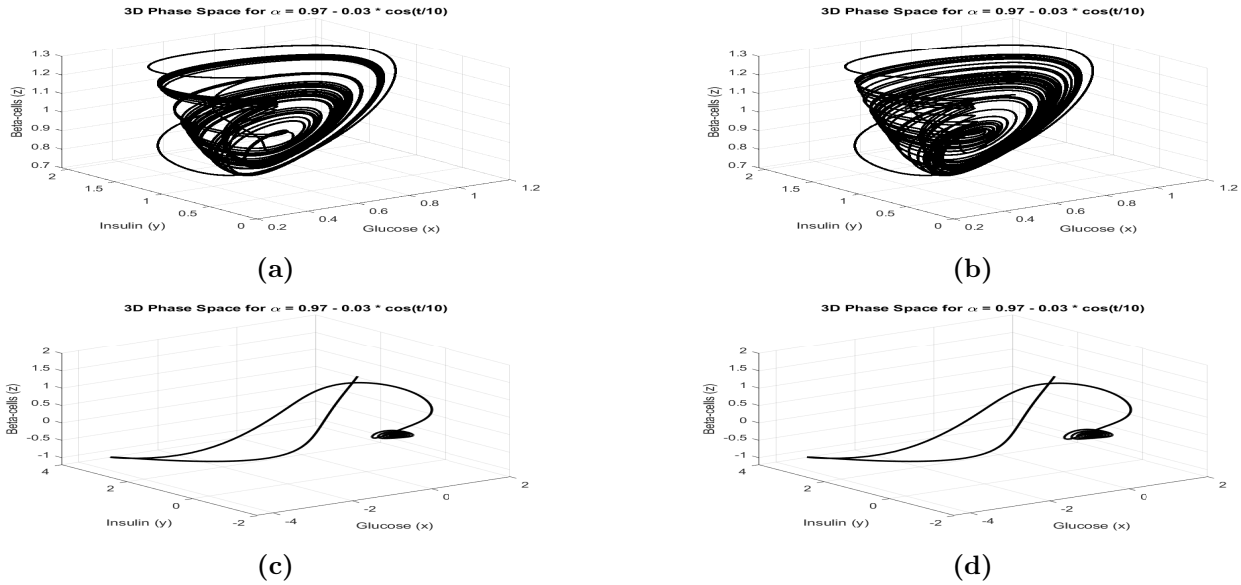

Figure 14. Compared between the 3D phases of (1) illustrated in (a), (b) and the controlled system (2) illustrated in (c), (d) under JSCSM and MSGDTM for $\alpha = 0.97 - 0.03 \times cos(t/10)$

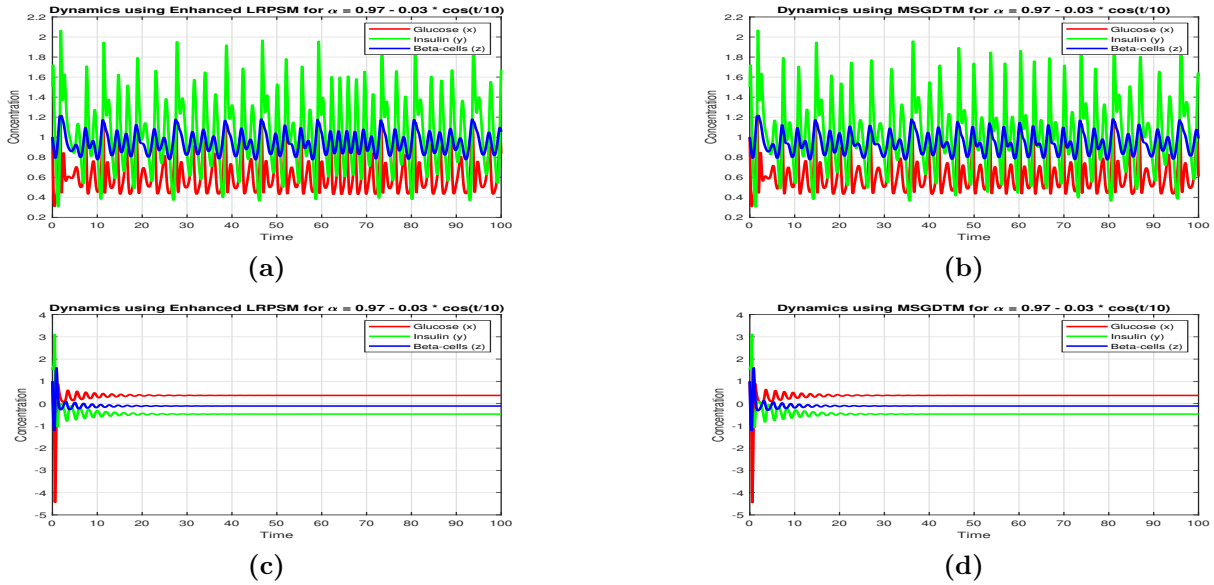

Figure 15. The time series of (1) shown in (a), (b) and the controlled system (2) shown in (c), (d) for $\alpha = 0.97 - 0.03 \times cos(t/10)$ under JSCSM and MSGDTM

uncontrolled and controlled scenarios at orders $\alpha = 1$ and $\alpha = 0.98$. In contrast, Figures 7 through 9 investigate more intricate fractional order variations, such as sinusoidal fluctuations ($\alpha = 0.97 - 0.03\sin(t/10)$), hyperbolic tangent adjustments ($\alpha = 0.97 + 0.03\tanh(t/10)$), and other time-dependent modifications. These visualizations reveal transitions between equilibrium, oscillatory dynamics, and chaotic behavior, underscoring the model's responsiveness to fractional order variations. Additionally, Figure 10 showcases a phase plane projection (xyz), providing a comparative visualization of system trajectories and attractor structures under different fractional orders and control strategies.

6. Discussion

This study presented a Model (1) to capture the memory-dependent and nonlinear behaviors inherent in metabolic control systems. Using the Caputo derivative framework, combined with two numerical schemes (MSGDTM and JSCSM), we explored how fractional-order dynamics and key parameters affect system stability, chaos, and control. This study explored a Model (1) by employing the following two numerical techniques: the MSGDTM and the JSCSM. The model incorporates memory-dependent Caputo fractional derivatives, allowing for more accurate simulation of real biological processes that exhibit hereditary

and nonlocal characteristics. Fractional-order glucose-insulin regulation is highlighted in this study. The model captures nonlocal and memory-dependent glucose-insulin interactions by incorporating fractional derivatives. This feature provides a more realistic representation of glucose regulation than traditional integer-order models. The behavior of the system is highly dependent on fractional orders and parameter variations. In healthy physiological states, fractional orders close to $\alpha = 1$ stabilize near equilibrium points. However, for $\alpha < 1$, the system exhibits oscillatory or chaotic behaviors, potentially mimicking pathological conditions like insulin resistance or glucose instability. This study provides valuable insights into how deviations in physiological conditions can lead to metabolic disorders and how fractional parameters influence system stability. The MSGDTM provides superior numerical accuracy, faster convergence, and greater computational efficiency compared to the JSCSM. It is particularly effective at handling nonlinear and memory-dependent characteristics of fractional glucose-insulin systems. As a result of lower approximation errors, MSGDTM is a more reliable method for solving fractional differential equations. Furthermore, this study explores how control mechanisms influence chaotic glucose-insulin dynamics. A controlled system exhibits significant improvements in stability, suggesting therapeutic interventions to prevent metabolic disorders. By using LE analysis and bifurcation diagrams, diabetes management strategies can be developed. Due to this, fractional-order modeling is becoming more important in biomedicine. Furthermore, it improves glucose-insulin dynamics to design therapeutic strategies for diabetes management. To improve real-world application, stochastic effects, environmental influences, or adaptive control strategies might be incorporated. Furthermore, integrating patient-specific data could enhance predictive modeling and optimize diabetes treatment.

7. Conclusion

In this work, we investigated a Model (1) incorporating Caputo fractional derivatives to capture memory effects and hereditary characteristics inherent in biological systems, particularly glucose-insulin interactions. Two advanced numerical techniques—the MSGDTM and the JSCSM—were employed to solve the model and analyze its dynamic behavior. Through comprehensive stability, bifurcation, and chaos analyses, we identified key parameters (a_{16} to a_{21}) that govern transitions between equilibrium, oscillatory, and chaotic dynamics, providing insights into mechanisms such as β-cell stress, insulin production, and glucose feedback. Numerical simulations demonstrated that MSGDTM outperforms JSCSM and other classical schemes in terms of accuracy, convergence speed, computational stability, and efficient handling of nonlocal memory terms, particularly in capturing nonlinear and oscillatory behaviors over long time intervals and near chaotic regimes. The bifurcation and Lyapunov analyses further confirmed that fractional-order models reflect more realistic physiological behavior compared to their integer-order counterparts, with graphical results emphasizing system sensitivity to fractional order variations ($\alpha = 0.97$ to 1.0) and validating the effectiveness of linear control strategies in stabilizing chaotic fluctuations. Based on these findings, fractional modeling is important in reproducing realistic glucose-insulin dynamics and informing improved diabetes treatment interventions. Although limitations remain—such as the restricted range of simulated fractional orders—the overall model remains biologically consistent, with negative parameters interpreted as inhibitory or decay processes. Looking ahead, we plan to extend the analysis to broader ranges of fractional orders, incorporate stochastic perturbations and time-delay effects, and integrate patient-specific clinical data to enhance the model's applicability for personalized treatment planning. This study highlights the value of fractional calculus and the robustness of MSGDTM as a powerful, adaptable tool for solving complex nonlinear biomedical systems.

Acknowledgments

The authors extend their appreciation to Umm Al-Qura University, Saudi Arabia, for supporting this research under Grant No. 25UQU4340608GSSR02.

Funding

This research work was funded by Umm Al-Qura University, Saudi Arabia, under Grant No. 25UQU4340608GSSR02.

Conflict of interest

The authors declare they have no competing interests.

Author contributions

Conceptualization: Sayed Saber, Brahim Dridi
Investigation: Sayed Saber, Abdullah Alahmari, Mohammed Messaoudi

Methodology: Sayed Saber
Formal analysis: Sayed Saber, Brahim Dridi
Writing–original draft: Abdullah Alahmari, Mohammed Messaoudi
Writing–review & editing: All authors

Availability of data

Not applicable.

AI tools statement

All authors confirm that no AI tools were used in the preparation of this manuscript.

References

1. Zabidi NA, Majid ZA, Kilicman A, et al. Numerical solution of fractional differential equations with Caputo derivative by using numerical fractional predict–correct technique. *Adv Cont Discr Mod.* 2022;2022:1-23.
2. Podlubny I. *Fractional Differential Equations.* San Diego: Academic Press; 1999.
3. Arena P, Caponetto R, Fortuna L, and Porto M. *Nonlinear Noninteger Order Circuits and Systems – An Introduction.* Singapore: World Scientific; 2000.
4. Nisar KS, Farman M, Abdel-Aty, Ravichandran C. A review of fractional-order models for plant epidemiology. *Prog Fract Differ Appl.* 2024;10:489-521.
5. Ahmed E, Elgazzar AS. On fractional order differential equations model for nonlocal epidemics. *Physica A.* 2007;379(2):607-614.
6. Li W, Wang Y, Cao J, Abdel-Aty M. Dynamics and backward bifurcations of SEI tuberculosis models in homogeneous and heterogeneous populations. *J Math Anal Appl.* 2025;543:128924.
7. Nisar KS, Farman M, Abdel-Aty M, Ravichandran C. A review of fractional order epidemic models for life sciences problems: past, present and future. *Alexandria Eng J.* 2024;95:283-305.
8. Bagley RL, Calico RA. Fractional order state equations for the control of viscoelastically damped structures. *J Guid Control Dyn.* 1991; 14:304-311.
9. Heaviside O. *Electromagnetic Theory.* New York: Chelsea Publishing Company; 1971.
10. Kusnezov D, Bulgac A, Dang GD. Quantum Lévy processes and fractional kinetics. *Phys Rev Lett.* 1999;82:1136-1139.
11. Almutairi N, Saber S. Existence of chaos and the approximate solution of the Lorenz–Lü–Chen system with the Caputo fractional operator. *AIP Adv.* 2024;14:015112.
12. Hilfer R. *Applications of Fractional Calculus in Physics.* Singapore: World Scientific; 2000:87-130.
13. Saber S. Control of chaos in the Burke-Shaw system of fractal-fractional order in the sense of Caputo-Fabrizio. *J Appl Math Comput Mech.* 2024;23(1):83-96.
14. Ahmed K, Adam H, Almutairi N, Saber S. Analytical solutions for a class of variable-order fractional Liu system under time-dependent variable coefficients. *Results Phys.* 2024;56:107311.
15. Almutairi N, Saber S. On chaos control of nonlinear fractional Newton-Leipnik system via fractional Caputo-Fabrizio derivatives. *Sci Rep.* 2023;13:22726.
16. Almutairi N, Saber S, and Ahmad H. The fractal-fractional Atangana-Baleanu operator for pneumonia disease: stability, statistical and numerical analyses. *AIMS Math.* 2023;8(12):29382-29410.
17. Almutairi N, Saber S. Chaos control and numerical solution of time-varying fractional Newton-Leipnik system using fractional Atangana-Baleanu derivatives. *AIMS Math.* 2023;8(11):25863-25887.
18. Petras I. *Fractional-Order Nonlinear Systems: Modeling, Analysis and Simulation.* Berlin: Springer; 2011.
19. Ahmed KIA, Adam HDS, Almutairi N, et al. Analytical solutions for a class of variable-order fractional Liu system under time-dependent variable coefficients. *Results Phys.* 2024;56:107311.
20. Alhazmi M, Dawalbait F, Aljohani A, et al. Numerical approximation method and chaos for a chaotic system in sense of Caputo-Fabrizio operator. *Thermal Sci.* 2024;28(6B):5161-5168.
21. Almutairi N, Saber S. Chaos control and numerical solution of time-varying fractional Newton-Leipnik system using fractional Atangana-Baleanu derivatives. *AIMS Math.* 2023;8:25863-25887.
22. Alsulami A, Alharb RA, Albbogami TM, et al. Controlled chaos of a fractal–fractional Newton-Leipnik system. *Thermal Sci.* 2024;28(6B).
23. Alshehri MH, Saber S, and Duraihem FZ. Dynamical analysis of fractional-order of IVGTT glucose–insulin interaction. *Int J Nonlin Sci Numer Simul.* 2023;24:1123-1140.
24. Alshehri MH, Duraihem FZ, Alalyani A, et al. A caputo (discretization) fractional-order model of glucose-insulin interaction: numerical solution and comparisons with experimental data. *J Taibah Univ Sci.* 2021;15:26-36.
25. Sayed Saber, Eihab Bashier, Alzahrani S., Noaman IA. A mathematical model of glucose-insulin interaction with time delay. *J. Appl Comput Math.* 2018;7(3):1-5.
26. Ahmed KIA, Adam HDS, Yousiff MY, et al. Different strategies for diabetes by mathematical modeling: applications of fractal-fractional derivatives in the sense of Atangana-Baleanu. *Results Phys.* 2023;26: 106892.
27. Ahmed KIA, Adam HDS, Yousiff MY, et al. Different strategies for diabetes by mathematical

modeling: modified minimal model. *Alexandria Eng J.* 2023;80:74-87.
28. Derouich M, Boutayeb A. The effect of physical exercise on the dynamics of glucose and insulin. *J Biomech.* 2002;35(7): 911–917.
29. Mukhopadhyay A, DeGaetano A, Arino O. Modeling the intravenous glucose tolerance test: a global study for a single-distributed-delay model. *Discrete Contin Dyn Syst Ser B.* 2004;228(4):407-417.
30. Tornheim K. Are metabolic oscillations responsible for normal oscillatory insulin secretion? *Diabetes.* 1997;46(9):1375-1380.
31. Dalla Man C, Caumo A, Basu R, Rizza R, Toffolo G, and Cobelli C. Minimal model estimation of glucose absorption and insulin sensitivity from oral test: Validation with a tracer method. *Am J Physiol Endocrinol Metab.* 2004;287(4):E637-E643.
32. Ahmed KIA, Mirgani SM, Seadawy A, et al. A comprehensive investigation of fractional glucose-insulin dynamics: existence, stability, and numerical comparisons using residual power series and generalized Runge–Kutta methods. *J Taibah Univ Sci.* 2025;19(1):1-15.
33. Naik PA, Yeolekar BM, Qureshi S, et al. Global analysis of a fractional-Order hepatitis B virus model under immune response in the presence of cytokines. *Adv Theory Simul.* 2024;7:2400726.
34. Saber S, Alalyani A. Stability analysis and numerical simulations of IVGTT glucose-insulin interaction models with two time delays. *Math Model Anal.* 2022;27:383-407.
35. Haroon DS, Mohammed A, Safa MM, et al. An application of Newton's interpolation polynomials to the zoonotic disease transmission between humans and baboons system based on a time-fractal fractional derivative with a power-law kernel. AIP Adv. 2025;15(4):045217.
36. Danca MF. Lyapunov exponents of a discontinuous 4D hyperchaotic system of integer or fractional order. *Entropy.* 2018;20(5):337.
37. Zhuang P, Liu F, Anh V, and Turner I. Numerical methods for the variable-order fractional advection-diffusion equation with a nonlinear source term. *SIAM J Numer Anal*, 2009;47(3):1760-1781.
38. Almutairi N, Saber S. Application of a time-fractal fractional derivative with a power-law kernel to the Burke-Shaw system based on Newton's interpolation polynomials. *MethodsX.* 2024;12:102510.
39. Gómez-Aguilar JF. Chaos in a nonlinear Bloch system with Atangana–Baleanu fractional derivatives. *Numer Methods Partial Differ Equ.* 2018;34(5):1716-1738.
40. Atangana A, Baleanu D. New fractional derivatives with non-local and non-singular kernel: theory and application to heat transfer model. *Thermal Sci.* 2016;20:763-769.
41. Caputo M, Fabrizio M. A new definition of fractional derivative without singular kernel. *Prog Fract Differ Appl.* 2015;1:73-85.
42. Nosrati K, Volos C. Bifurcation analysis and chaotic behaviors of fractional-order singular biological systems. In: Pham VT, Vaidyanathan S, Volos C, Kapitaniak T, eds.*Nonlinear Dynamical Systems with Self-Excited and Hidden Attractors* Studies in Systems, Decision and Control, vol. 133. Cham:Springer; 2018.
43. Odibat ZM, Momani S. Modified homotopy perturbation method: application to quadratic Riccati differential equation of fractional order. *Chaos Solitons Fractals.* 2008;36:167-174.
44. Tsai P, Chen CK. An approximate analytic solution of the nonlinear Riccati differential equation. *J Franklin Inst.* 2010;347: 1850-1862.
45. Zeng DQ, Qin YM. The Laplace-Adomian-Padé technique for the seepage flows with the Riemann–Liouville derivatives. *Commun Fract Calc.* 2012;3:26-29.
46. Khan Y, Diblík J, Faraz N, Smarda Z. An efficient new perturbative Laplace method for space-time fractional telegraph equations. *Adv Differ Equ.*, 2012;2012:204.
47. Khan NA, Ara A, Khan NA. Fractional-order Riccati differential equation: analytical approximation and numerical results. *Adv Differ Equ.*, 2013;2013:185.
48. Odibat Z, Momani S. An algorithm for the numerical solution of differential equations of fractional order. *J Appl Math Inform.* 2008;26:15-27.
49. Kataria KK, Vellaisamy P. Saigo space–time fractional Poisson process via Adomian decomposition method. *Stat Probab Lett.* 2017;129:69-80
50. Haq F, Shah K, Rahman GU, Shahzad M. Numerical solution of fractional-order smoking model via Laplace-Adomian decomposition method. *Alexandria Eng J.* 2018;57:1061-1069.
51. Sirisubtawee S, Kaewta S. New modified Adomian decomposition recursion schemes for solving certain types of nonlinear fractional two-point boundary value problems. *Int J Math Math Sci.* 2017;2017:1–20.
52. Liu Q, Liu J, Chen Y. Asymptotic limit cycle of fractional Van der Pol oscillator by homotopy analysis method and memory-free principle. *Appl Math Model.* 2016;40(4): 3211-3220.
53. Freihat A, Momani S. Application of multistep generalized differential transform method for the solutions of the fractional-order Chua's system. *Discrete Dyn Nat Soc.* 2012;2012:1–13.
54. Wang H, Yang D, Zhu S. A Petrov–Galerkin finite element method for variable-coefficient fractional diffusion equations. *Comput Methods Appl. Mech Eng.* 2015;290:45-56.

55. Song H, Yi M, Huang J, Pan Y. Numerical solution of fractional partial differential equations by using Legendre wavelets. *Eng Lett.* 2016;24(3):358-364.
56. Lu H, Bates PW, Chen W, Zhang M. The spectral collocation method for efficiently solving PDEs with fractional Laplacian. *Adv Comput Math.* 2017;44(6):861–878.
57. Odibat Z, Momani S, Erturk VS. Generalized differential transform method: Application to differential equations of fractional order. *Appl Math Comput.* 2008;197(2):467-477.
58. Momani S, Odibat Z. A novel method for nonlinear fractional partial differential equations: Combination of DTM and generalized Taylor's formula. *J Comput Appl Math.* 2008;220(1–2):85-95.
59. Odibat Z, Momani S. A generalized differential transform method for linear partial differential equations of fractional order. *Appl Math Lett.* 2008;21(2):194-199.
60. Erturk VS, Momani S, Odibat Z. Application of generalized differential transform method to multi-order fractional differential equations. Commun Nonlinear Sci Numer Simulat. 2008;13(8):1642-1654.
61. Odibat ZM, Bertelle C, Aziz-Alaoui MA, Duchamp GHE. A multi-step differential transform method and application to non-chaotic or chaotic systems. Comput $\mathcal{E}$ Math Appl. 2010;59(4):1462-1472.
62. Ertürk VS, Odibat ZM, Momani S. An approximate solution of a fractional order differential equation model of human T-cell lymphotropic virus I (HTLV-I) infection of CD4 4^{+}T-cells. Comput E Mathem Appl 2011;62(3):996-1002.
63. Odibat ZM, Bertelle C, Aziz-Alaoui MA, Duchamp GHE. A multistep differential transform method and application to non-chaotic or chaotic systems. Comput Mathemat Appl. 2010;59(4):1462-1472.
64. Erturk VS, Odibat ZM, Momani S. An approximate solution of a fractional order differential equation model of human T-cell lymphotropic virus I (HTLV-I) infection of CD4 T-cells. Comput Math Appl. 2011;62(3):996– 1002.
65. Asad Freihat A, Momani S. Application of multistep generalized differential transform method for the solutions of the fractional-order chua's system. Discrete Dyn Nat Soc. 2012; 2012:427393.
66. Liu C-S. Counterexamples on Jumarie's three basic fractional calculus formulae for non-differentiable continuous functions. Chaos Solit Fract. 2018;109:219-222.
67. . Odibat Z, Momani S, Erturk VS. Generalized differential transform method: application to differential equations of fractional order. Appl Math Comput. 2008;197(2):467–477.
68. Joshi H, Yavuz M, Taylan O, Alkabaa A. Dynamic analysis of fractal-fractional cancer model under chemotherapy drug with generalized Mittag-Leffler kernel. Comput Methods Programs Biomed. 2025;260:108565.
69. Gundogdu H, Joshi H. Numerical analysis of time-fractional cancer models with different types of net killing rate. Mathemat. 2025; 13:536.
70. Hardik J. Mechanistic insights of COVID-19 dynamics by considering the influence of neurodegeneration and memory trace. Physica Scrip. 2024;99(3):35254.
71. Joshi H, Jha BK. Generalized diffusion characteristics of Calcium model with concentration and memory of cells: a spatiotemporal approach. Iran J Sci Technol Trans Sci. 2022;46:309–322.
72. Yavuz M, Mur R, Yildiz M, Joshi H. Mathematical modeling of middle east respiratory syndrome coronavirus with bifurcation analysis. Contemp Math [Internet]. 2024;5(3):3997-4012.
73. Erturk V, Zaman G, Momani S. A numeric analytic method for approximating a giving up smoking model containing fractional derivatives. Comput $\mathcal{E}$ Math Appl. 2012;64(10):3065-3074.
74. Elsadany AEA, El-Metwally HA, Elabbasy EM, et al. Chaos and bifurcation of a nonlinear discrete preypredator system. Comput Ecol Softw. 2012; 2(3):169-180.
75. Shabestari PS, Panahi S, Hatef B, et al. A new chaotic model for model (1). Chaos Sol Fract. 2018;112:44-51.

Sayed Saber *Sayed Saber is a Professor of Mathematics at Al-Baha University, Saudi Arabia, and Beni-Suef University, Egypt. His research interests span several complex variables, fractional calculus, chaos theory, and advanced computational methods with a focus on biomedical systems. He has published extensively in the areas of complex analysis and applied mathematics, with a particular emphasis on nonlinear dynamics and fractional differential equations. Prof. Dr. Saber has made significant contributions to the development and analysis of advanced techniques for solving D-bar equations on complex manifolds and investigating complex systems behavior. He is also recognized for his pioneering work in chaos control and fractional-order modeling, especially in biomedical and epidemiological applications.*

https://orcid.org/0000-0002-5790-3222

Brahim Dridi *Brahim Dridi is an Associate Professor of Mathematics at Umm Al-Qura University in Makkah, Saudi Arabia. His research centers on partial differential equations, with a focus on nonlinear problems involving exponential and logarithmic weights, as well as Kirchhoff-type equations. He has published extensively in peer-reviewed journals such as Mediterranean Journal of Mathematics, Mathematische Nachrichten, and Acta Applicandae Mathematicae. His recent work explores critical exponential growth, N-Laplacian equations, and sign-changing solutions in weighted frameworks. Dr. Dridi actively*

collaborates with researchers internationally.
https://orcid.org/0000-0001-5863-029X

Abdullah Alahmari *Dr. Abdullah Alahmari is a faculty member in the Mathematics Department at Umm Al-Qura University, Saudi Arabia. His research focuses on operator theory and functional analysis, with a growing interest in complex analysis. In functional analysis, his central interests are the study of spaces of functions, and more generally of topological vector spaces and their associated structures by means of topological, analytical and geometric methods, the study of Banach algebras, and the calculus of variations, especially variational convergence.*
https://orcid.org/0000-0002-9596-910X

Mohammed Messaoudi *Dr Mohammed Messaoudi holds a PhD degree in computer science from the University of Durham, United Kingdom. He has extensive experience in both industry and academia in UK, Canada and Saudi Arabia. He is currently working as an assistant professor at Imam Mohammad Ibn Saud Islamic University. Research area: Software Requirements engineering, optimization, and Modelling and Simulation.*
https://orcid.org/0009-0005-2954-1753

An International Journal of Optimization and Control: Theories & Applications
(https://accscience.com/journal/ijocta)